# ORBITAL DOCKING GUIDANCE SYSTEM USING GAMMA RADIATION

by

John Albert Sorensen

A Thesis Submitted to the

Graduate Faculty in Partial Fulfillment of

The Requirements for the Degree of

MASTER OF SCIENCE

Major Subject: Theoretical and Applied Mechanics



Iowa State University
Of Science and Technology
Ames, Iowa

1964

# TABLE OF CONTENTS

# INTRODUCTION

A space project which has been receiving increasing consideration recently in this country is the concept of establishing a permanent, manned space laboratory orbiting the earth. In general, capabilities of such a satellite will include the abilities of "growing", maintaining a constant position, and changing to a new position when desired. Useful tasks that the satellite might be expected to perform include weather observation, space exploration, communications, and enemy observation.

There are several factors which create a need for a system of ferry vehicles to operate between the earth and such a satellite. In the first place, a satellite of the versatility described would be a complex structure, too large to launch from the earth in one unit. Ferry vehicles would allow the satellite to be launched gradually in several parts and to be assembled in space. Also, because the satellite will be manned (at least part of the time) and will have position control engines and other equipment on board, ferry vehicles are needed to convey the men and necessary fuel, parts, and other supplies to and from the satellite when required.

The problem of launching and guiding a ferry vehicle, or interceptor, to an orbiting satellite is complex and of large scale in itself. It is best handled by separation into four phases that are designated as launch, midcourse guidance, terminal guidance, and docking. There is a great deal of interdependence among these phases, but for preliminary investigation it is convenient to treat each separately.

The launch phase is self-explanatory, being simply the ascent of

the interceptor from earth into space. The middle two phases, midcourse and terminal guidance, are generally referred to as space rendezvous. During these phases the interceptor is brought "near" the orbiting satellite. The final maneuver, docking, is concerned with the actual joining of the interceptor with the satellite, or target. Docking is of particular importance, for a soft, accurate union of the two vehicles is essential if the transmission of delicate cargo is to be successfully accomplished. This final docking phase is the subject of this research.

Docking differs from rendezvous because the scale of distances and velocities is finer. Another factor also gains importance in the docking phase, for the target can no longer be treated as a point in space by the interceptor. Instead, its attitude, or relative angular alignment to the interceptor, must be sensed and considered. These factors create a need for a more accurate short-range guidance system than is considered necessary for the rendezvous phase. Studies have shown that this need can most easily be met by using the visual abilities of man (11). However, there are many instances, particularly in the early stages of construction of the satellite, when man's presence would be otherwise unnecessary. Also, after the space station is operational, only occasional servicing visits by man might be necessary, while more frequent supply deliveries will be required. Thus, it would be highly desirable to have an automatic docking system by which the interceptor and target could be successfully united regardless of the presence or absence of man.

Current knowledge indicates that radar is the most applicable system that can be used for range and relative velocity determination

when both quantities are large. Therefore, the guidance system used by the interceptor during the rendezvous phase will probably be an on-board radar tracking system. However, there is a minimum range point after which radar sensor data lacks the accuracy necessary to guide close maneuvers. This loss of accuracy is due to the nearness of the target to the antenna and to the transponder time delay. A second limitation of radar is that it cannot determine the attitude of the target but must treat it simply as a point in space. Therefore, the docking maneuver cannot be successfully guided by the radar guidance system used during rendezvous. It will thus be the purpose of this paper to make a preliminary investigation of an automatic docking system by which the docking maneuver can be precisely controlled.

In general, this docking guidance system will be required to steer the interceptor from any random direction to the line of approach which is favorable for docking. After the interceptor reaches the desired line of approach, it must be kept on that line and move at a specified velocity until docking is complete. Thus, at given time intervals during the docking maneuver, the guidance system on the interceptor must measure relative velocity components and generate steering commands to correct velocity errors as required. The interceptor is assumed to approach the target from the rear at a relative closing velocity that is less than 20 feet per second when the range is 1500 feet.

There are various estimates of the measurement errors that would be present in the radar systems that are available for rendezvous guidance. Heilfron and Kaufman (7, p. 248) assumed that the radar measurement errors of range and relative velocity would be $\pm 0.1\%$ $\pm 5$ feet and $\pm 0.5$

feet per second, respectively. Wolverton (21, p. 4-127) said these same errors would be less than ±50 feet and ±2.25 feet per second. For the purposes of this paper, the accuracy of the rendezvous radar guidance system's range and relative velocity measurements are assumed to be ±10 feet and ±1 foot per second. They are assumed acceptable until a range of 500 feet is reached at which time the docking guidance system will begin making these measurements. The attitude measurements must necessarily begin sooner than this, however. Therefore, this part of the docking system will begin functioning when the range between the interceptor and target is 1500 feet.

In this study, the target is treated as being a "passively cooperative" vehicle. In other words, it does not maneuver during the docking phase nor send radio commands to guide the interceptor.

The guidance system investigated utilizes the principles of gamma-ray detection and identification by means of a scintillation detector. Point sources of gamma-ray photons located on the target are detected by scintillation detectors mounted on the interceptor. Using the relative source positions and signal strengths of the gamma radiation, the interceptor is able to determine the range and attitude of the target. Using these values and their rates of change with respect to time, the interceptor guides itself to the target.

The first part of the ensuing discussion is concerned with deriving the equations of relative motion between the two vehicles in terms of a cartesian coordinate system, with the origin established on the target vehicle. The method of trigonometric determinations of the relative position and velocity components is included. The second part of the

investigation deals with the use of the scintillation detector for gamma-ray detection. It is shown that this method of gamma-ray detection can be applied both for determination of the attitude angles and the range. Finally, it is demonstrated that relative velocity and position equations and the values of range and attitude can be applied to control the docking maneuver. It is also shown that the interceptor can be guided along any desired approach line to the target and that the relative closing velocity can be controlled as desired.

## LIST OF SYMBOLS

| | |
|---|---|
| A | area |
| AM | atomic mass |
| c | radius of the scintillation detector's phosphor crystal |
| $C_1$ | constant value of position coordinate |
| $C_2$ | constant value of relative velocity component |
| $\bar{e}_i, \bar{e}_j, \bar{e}_k$ | unit vectors in the X, Y, and Z directions |
| FM | line formed by the two points F and M |
| $\angle$FMK | angle formed by lines FM and MK |
| k | gain constant |
| $l_1$, $l_2$ | lengths of the sides of JKLMJ |
| J,K,L,M, | point sources of gamma radiation on the target |
| JKLMJ | rectangle formed by the four points |
| JKFJ | triangle formed by the three points |
| $m_p$ | mass of the interceptor |
| n | ratio of the number of photons detected to the number emitted |
| N | number of particular radioactive atoms present at any one time |
| $N_o$ | original number of radioactive atoms present |
| P | interceptor |
| r | range between the interceptor and the target |
| r' | radial distance from the orbit center to the interceptor |
| R | radius of the spherical point source |
| R' | radial distance from the orbit center to the target |
| S | target |
| t | time |

| | |
|---|---|
| $T$ | half-life of a radioactive material |
| $T'$ | time period allowed for docking |
| $T_x, T_y, T_z$ | thrust in the X, Y, and Z directions |
| $v$ | relative velocity of the interceptor |
| $V_e$ | error margin velocity |
| $x, y, z$ | components of r in the X, Y, and Z directions |
| $X, Y, Z$ | axes of cartesian coordinate system established on the target |
| $\alpha, \beta, \gamma$ | angles formed between the sensors as they point toward the point sources |
| $\Delta$ | small increment |
| $\Psi$ | angle between vectors $\bar{r}'$ and $\bar{R}'$ |
| $\Theta$ | angle between the X axis and the line-of-sight between the two vehicles |
| $\lambda$ | decay constant of a material |
| $\mu$ | cone half-angle |
| $\sigma$ | standard deviation from the mean |
| $\phi$ | angle between the XY plane and the rX plane |
| $\omega$ | angular velocity of the target |

Subscripts

| | |
|---|---|
| i | ideal value |
| tot | total |
| o | original value |
| l | final value |

Special Notation

| | |
|---|---|
| $\dot{x}$ | the dot denotes a time derivative of x |
| $\ddot{x}$ | the two dots denote the second derivative of x |

$\bar{x}$ the bar denotes a vector

$>$ is greater than

$\approx$ nearly equal to

## RELATIVE MOTION AND ITS MEASUREMENT

### Velocity and Acceleration Equations

In this investigation the target vehicle can be described as traveling in an elliptical path about the earth. This path is determined by ground tracking equipment before the interceptor is launched. During the period of docking, the elliptical path can be assumed to consist of a circular arc. That is, during the docking maneuver, the target vehicle is treated as traveling in a circular path with a constant angular velocity $\bar{\omega}$.

The axis system used is shown in Figure 1. The X axis is in the direction of the target motion along its circular path, the Z axis points toward the orbit center, and the Y axis is orthogonal to both X and Z. The interceptor vehicle will likewise have three orthogonal axes. The longitudinal axis of the interceptor is arbitrarily defined as the axis which is aligned parallel to the target X axis when docking is complete. This is called the roll axis. The other two axes of the interceptor, which will be parallel to the target Y and Z axes upon docking completion, are known as pitch and yaw axes respectively.

In Figure 1 the velocity of the interceptor P is

$$\dot{\bar{r}}' = \dot{\bar{R}}' + \dot{\bar{r}} \tag{1}$$

$$= \dot{\bar{R}}' + \bar{\omega} \times \bar{r} + \bar{v} \tag{2}$$

where $\bar{v}$ is the velocity of P with respect to the cartesian coordinate system established at the target S. The relative velocity of the interceptor to the target satellite is

$$\dot{\bar{r}} = \bar{\omega} \times \bar{r} + \bar{v} \ . \tag{3}$$

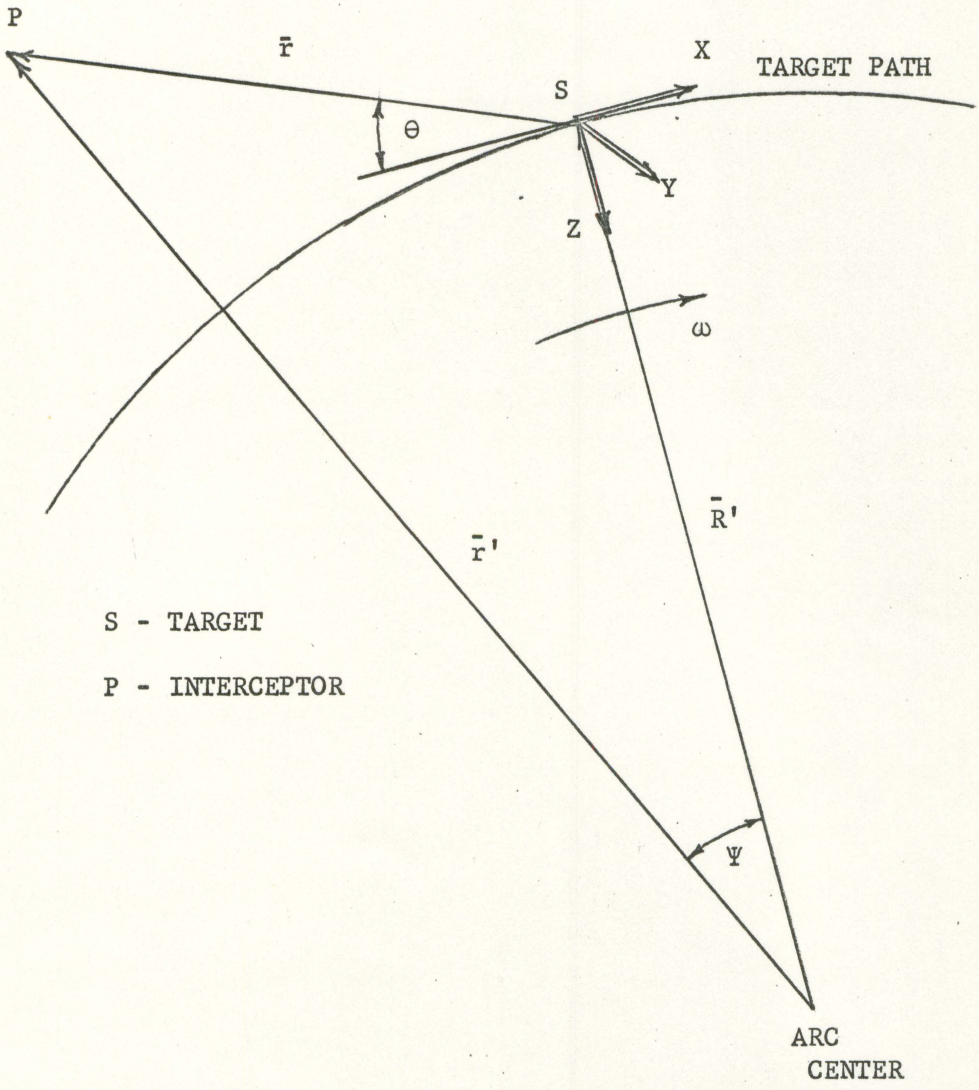


Figure 1. Geometry of problem showing target based axis system

Now $\bar{e}_i$, $\bar{e}_j$, and $\bar{e}_k$ are defined as being unit vectors in the X, Y, and Z directions respectively. Then

$$\bar{\omega} = -\omega \bar{e}_j \ , \tag{4}$$

$$\bar{r} = x\bar{e}_i + y\bar{e}_j + z\bar{e}_k \ , \tag{5}$$

$$\bar{v} = \dot{x}\bar{e}_i + \dot{y}\bar{e}_j + \dot{z}\bar{e}_k \ . \tag{6}$$

Using these relationships

$$\dot{\bar{r}} = (\dot{x} - \omega z)\bar{e}_i + \dot{y}\bar{e}_j + (\dot{z} + \omega x)\bar{e}_k \ . \tag{7}$$

Relative acceleration is (8)

$$\ddot{\bar{r}} = (\dot{x} - \omega z)\dot{\bar{e}}_i + (\ddot{x} - \omega \dot{z})\bar{e}_i + \dot{y}\bar{e}_j + (\dot{z} + \omega x)\dot{\bar{e}}_k + (\ddot{z} + \omega \dot{x})\bar{e}_k .$$

Now

$$\Delta \bar{e}_i = \bar{e}_k \omega \, \Delta t , \tag{9a}$$

$$\Delta \bar{e}_k = -\bar{e}_i \omega \, \Delta t , \tag{9b}$$

so

$$\dot{\bar{e}}_i = \omega \bar{e}_k , \tag{10a}$$

$$\dot{\bar{e}}_k = -\omega \bar{e}_i . \tag{10b}$$

Then

$$\ddot{\bar{r}} = (\ddot{x} - 2\omega \dot{z} - \omega^2 x)\bar{e}_i + \ddot{y}\bar{e}_j + (\ddot{z} + 2\omega \dot{x} - \omega^2 z)\bar{e}_k \ . \tag{11}$$

This acceleration is equal to the resultant thrust per unit mass on the interceptor vehicle. Because the angle $\Psi$ is very small and the difference in distances $\bar{R}'$ and $\bar{r}'$ is small compared to their overall length, the differential effects of gravity on the two vehicles is assumed negligible. During docking it can be assumed that the thrust levels will be small so that change in mass of the interceptor is also negligible. Then

$$\frac{T_x}{m_p} = \ddot{x} - 2\omega\dot{z} - \omega^2 x \ , \tag{12}$$

$$\frac{T_y}{m_p} = \ddot{y} \ , \tag{13}$$

$$\frac{T_z}{m_p} = \ddot{z} + 2\omega\dot{x} - \omega^2 z \ , \tag{14}$$

where $T_x$, $T_y$, and $T_z$ are the directional thrusts and $m_p$ is the interceptor's mass.

## Measurement of Relative Position and Velocity

The angular rate $\bar{\omega}$ is known to the interceptor. Then to determine what position changes the interceptor must make to dock, it must be able to measure the relative positions x, y, and z and the relative velocities $\dot{x}$, $\dot{y}$, and $\dot{z}$. Quantities x, y, and z are shown in Figure 2a where it is seen that for the interceptor in the position shown

$$x = -r \cos\theta \ , \tag{15}$$

$$y = -r \sin\theta \cos\phi \ , \tag{16}$$

$$z = -r \sin\theta \sin\phi \ , \tag{17}$$

in which $\theta$ is the angle between the X axis on the target and the line-of-sight between the two vehicles, and $\phi$ is the angle between the XY plane of the target vehicle and the plane defined by r and X.

In order to measure positions and velocities in the XYZ cartesian coordinate system, one must be able to measure r, $\theta$, and $\phi$ in the spherical coordinate system defined in Figure 2a. These quantities can be measured by placing four point sources of gamma-ray emitting material on the target in a rectangular pattern as shown in Figure 2b. These points are designated J, K, L, and M. Each point source is selected to

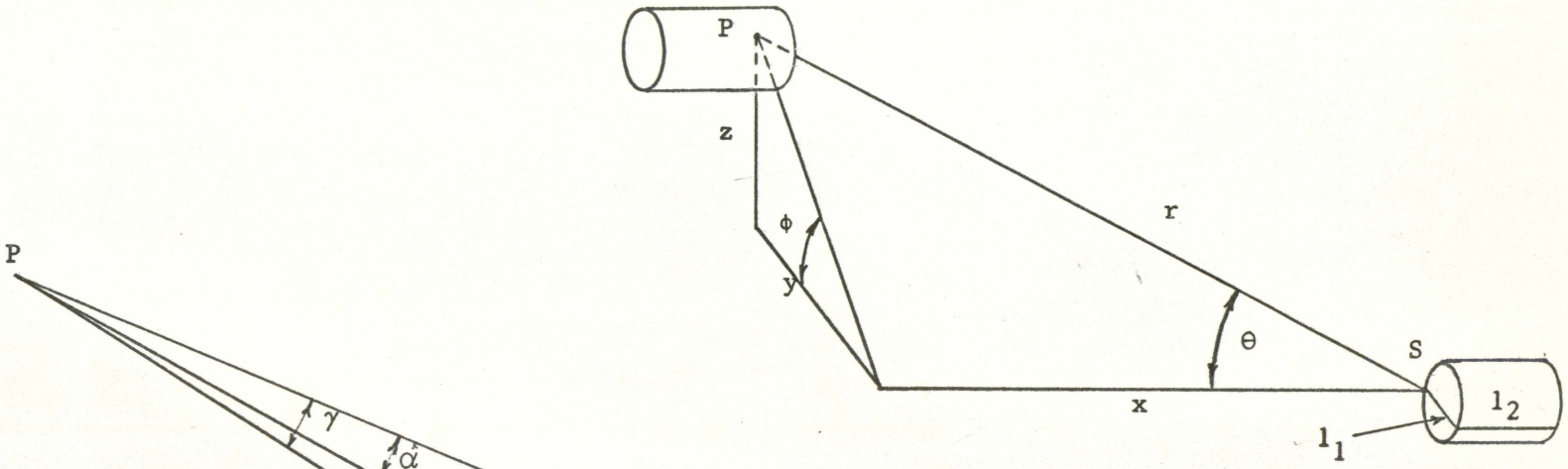


Figure 2a. x, y, and z components of r

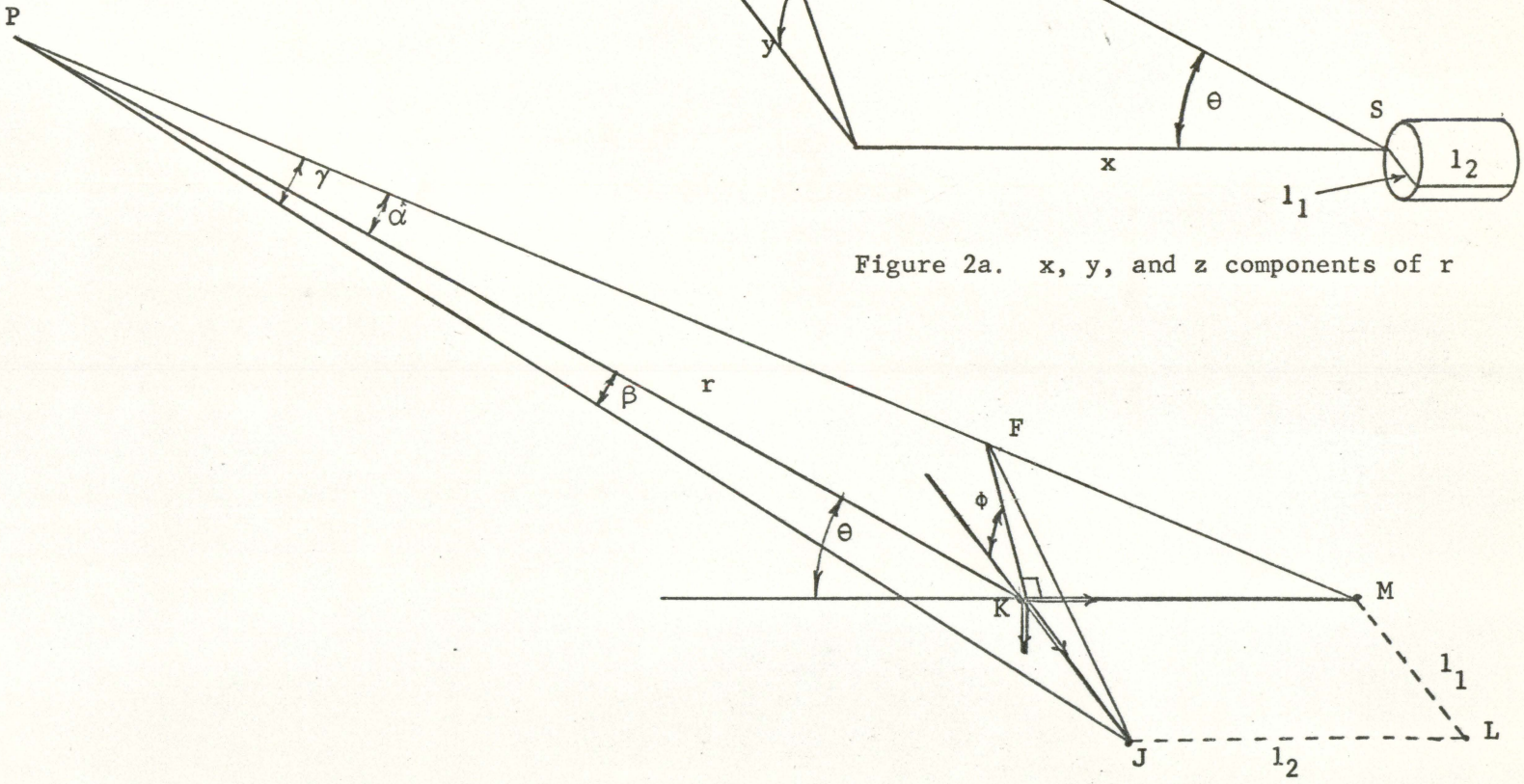


Figure 2b. Location of radiation point sources and the parameters they define

emit gamma rays of a different characteristic energy level so that it can be distinguished from the other three sources.

It is recognized that the rectangle JKLMJ forms a unique pattern as viewed from the interceptor vehicle. The interceptor is equipped with independent sensors, each seeking out and following only the point source with the energy level to which the sensor is "tuned". Then the positions of these gimbaled sensors along with the measured range enables the interceptor to compute the angles $\theta$ and $\phi$.

To compute $\theta$ and $\phi$ the geometry shown in Figure 2b is used. The lengths $l_1$ and $l_2$ are known. The range r and the angles $\alpha$, $\beta$, and $\gamma$ between the sensors are measured by the interceptor. By the sine law

$$\frac{\sin \alpha}{l_2} = \frac{\sin \angle FMK}{r} , \tag{18}$$

$$\angle FMK = \sin^{-1}\left(\frac{r}{l_2} \sin \alpha\right). \tag{19}$$

Then

$$\begin{aligned} \theta &= \alpha + \angle FMK \\ &= \alpha + \sin^{-1}\left(\frac{r}{l_2} \sin \alpha\right). \end{aligned} \tag{20}$$

Again using the sine law

$$\frac{\sin (180^\circ - \theta)}{MP} = \frac{\sin \alpha}{l_2} , \tag{21}$$

$$MP = \frac{l_2 \sin \theta}{\sin \alpha} . \tag{22}$$

Because

$$\sin \angle FMK = \frac{FK}{FM} , \tag{23}$$

and

$$\cos \angle FMK = \frac{KM}{FM} = \frac{l_2}{FM} , \tag{24}$$

then

$$FM = l_2 \sec \angle FMK$$

$$= l_2 \sec \left[ \sin^{-1} \left( \frac{r}{l_2} \sin \alpha \right) \right], \tag{25}$$

and

$$FK = FM \sin \angle FMK$$

$$= l_2 \tan \left[ \sin^{-1} \left( \frac{r}{l_2} \sin \alpha \right) \right]. \tag{26}$$

Now

$$FP = MP - FM. \tag{27}$$

Then from Equations 22 and 25

$$FP = \frac{l_2 \sin \theta}{\sin \alpha} - l_2 \sec \left[ \sin^{-1} \left( \frac{r}{l_2} \sin \alpha \right) \right]. \tag{28}$$

Again using the sine law

$$\frac{\sin \beta}{l_1} = \frac{\sin \angle KJP}{r} . \tag{29}$$

Then

$$\angle KJP = \sin^{-1} \left( \frac{r}{l_1} \sin \beta \right). \tag{30}$$

From this relationship

$$\angle JKP = 180^\circ - (\beta + \angle KJP). \tag{31}$$

Therefore,

$$JP = \frac{\sin \angle JKP}{\sin \beta} \; l_1$$

$$= \frac{\sin (\beta + \angle KJP)}{\sin \beta} \; l_1$$

$$= \frac{l_1}{\sin \beta} \sin \left[ \beta + \sin^{-1} \left( \frac{r}{l_1} \sin \beta \right) \right]. \tag{32}$$

From the cosine law

$$FJ = \sqrt{(FP)^2 + (JP)^2 - 2(FP)(JP)\cos\gamma} \quad . \tag{33}$$

The sides of the triangle JKFJ are now known. Again using the law of cosines

$$\angle JKF = \cos^{-1}\left[\frac{(JK)^2 + (FK)^2 - (FJ)^2}{2(JK)(FK)}\right]. \tag{34}$$

Finally,

$$\phi = 180^\circ - \angle JKF \quad . \tag{35}$$

The relationships developed in Equations 20, 26, 28, 30, 31, 32, 33, 34, and 35 are used to evaluate the angle $\phi$.

$$\phi = 180^\circ - \cos^{-1}\left\{\frac{l_1}{2\,l_2\tan\left[\sin^{-1}\left(\frac{r}{l_2}\sin\alpha\right)\right]} + \frac{l_2\tan\left[\sin^{-1}\left(\frac{r}{l_2}\sin\alpha\right)\right]}{2\,l_1}\right.$$

$$- \frac{\left[\frac{l_2\sin\left(\alpha + \sin^{-1}\left\{\frac{r}{l_2}\sin\alpha\right\}\right)}{\sin\alpha} - l_2\sec\left(\sin^{-1}\left\{\frac{r}{l_2}\sin\alpha\right\}\right)\right]^2}{2\,l_1 l_2\tan\left[\sin^{-1}\left(\frac{r}{l_2}\sin\alpha\right)\right]}$$

$$- \frac{\left[\frac{l_1\sin\left(\beta + \sin^{-1}\left\{\frac{r}{l_1}\sin\beta\right\}\right)}{\sin\beta}\right]^2}{2\,l_1 l_2\tan\left[\sin^{-1}\left(\frac{r}{l_2}\sin\alpha\right)\right]}$$

$$\left. + \cos\gamma\,\frac{\left[\frac{\sin\left(\alpha + \sin^{-1}\left\{\frac{r}{l_2}\sin\alpha\right\}\right)}{\sin\alpha} - \sec\left(\sin^{-1}\left\{\frac{r}{l_2}\sin\alpha\right\}\right)\right]\left[\frac{\sin\left(\beta + \sin^{-1}\left\{\frac{r}{l_1}\sin\beta\right\}\right)}{\sin\beta}\right]}{\tan\left[\sin^{-1}\left(\frac{r}{l_2}\sin\alpha\right)\right]}\right\}. \tag{36}$$

Equations 20 and 36 permit the evaluation of $\theta$ and $\phi$.

Considering Figure 2a and Equations 20 and 36 it is seen that four quantities (range r and angles $\alpha$, $\beta$, and $\gamma$) provide adequate information for computing the coordinate components x, y, and z. It is seen from Figure 2b that when the interceptor approaches the target from the left (the -Y direction), range r is measured between the interceptor and point K on the target. When the interceptor approaches from the right (the +Y direction), range r is measured between the interceptor and point J on the target.

The angles $\alpha$, $\beta$, and $\gamma$ are determined by sensors following points J, K, and M when the interceptor approaches from the left. These angles are determined by following points J, K, and L when the approach is from the right, because from this side, point M cannot be seen.

Hence, only three of the points on the target are required for position determination at one time. Thus, three sensors are required on the left side of the interceptor for position determination when the approach is from the left. The sensor following point K also determines range. Likewise, there must be three sensors on the right side of the interceptor for position determination when the approach is from the right. Then the sensor following point J also determines range.

It follows that the interceptor must be equipped with six sensors. Two of these sensors are designed to determine both range and point directions. When the approach is from the left, point K is the coordinate origin and line KM is the X axis. When the approach is from the right, line JL is the X axis with point J being the origin. The sensors on the interceptor are automatically turned on and off so that only the required three function at one time. The two groups of three sensors

on the interceptor are a distance $l_1$ apart, equal to the distance between points J and K on the target.

It is known from rigid body dynamics that six quantities are required to define the relative position of one rigid body to another. In this case, four of the six quantities are the range r, and the angles $\alpha$, $\beta$, and $\gamma$. The other two quantities are the angles formed by the pitch and yaw axes of the interceptor to the line-of-sight direction.

## MEASUREMENT OF PARAMETERS USING THE SCINTILLATION DETECTOR

### Principles of Nuclear Radiation

For a given radioactive material, every nucleus has a definite probability of decaying in a unit time. If N is the number of the particular atoms present at any time, the decay rate is

$$\dot{N} = -\lambda N \ , \tag{37}$$

where $\lambda$ is called the decay constant of that material. From this expression it is found that when the number of radioactive nuclei of a specified kind is originally $N_o$, the number left at time t later is

$$N = N_o \, e^{-\lambda t} . \tag{38}$$

By letting N equal one-half $N_o$, the half-life T of the radioactive material is found to be

$$T = \frac{\ln 2}{\lambda} = \frac{0.693}{\lambda} \ , \tag{39}$$

so the half-life is inversely proportional to the decay constant of the material.

Radioactive isotopes of four different energy levels are chosen as the four gamma-ray sources on the target vehicle. Because it is desired that the number of gamma photons emitted per second be fairly constant from day to day, materials with long half-lives are chosen. When a material with a certain half-life is chosen its decay constant $\lambda$ can be calculated from Equation 39. Then if the number of photons emitted per second is established, the number of atoms of the particular material can be calculated by Equation 37. Multiplying the resultant number of atoms N by the atomic mass (AM) of the material and dividing by Avogadro's

number ($6 \times 10^{23}$) gives the required mass of the material in grams.

$$\frac{(\dot{N})\ T\ (AM)}{(0.693)(6\times10^{23})} = \text{grams of material.} \tag{40}$$

Another quantity called the specific activity is used to express the rate at which unit weight of radioactive materials decay. This is the curie, and is defined as the quantity of material giving $3.70 \times 10^{10}$ disintegrations per second. This designation is required when considering what shielding is required to protect the target vehicle from the radioactive materials.

A table of suitable radioactive isotopes follows.

Table 1. Suitable radioactive isotopes

| Atomic Number | Isotope | Half Life (years) | Energy (Mev.) | Mass Required (grams) | Curies |
|---|---|---|---|---|---|
| 6 | $C^{15}$ | 5700 | 0.155 | $6.49 \times 10^{-2}$ | 0.2703 |
| 11 | $Na^{22}$ | 2.6 | 1.28 | $4.34 \times 10^{-5}$ | 0.2703 |
| 30 | $Zn^{65}$ | 0.685 | 1.114 | $3.38 \times 10^{-5}$ | 0.2703 |
| 36 | $Kr^{85}$ | 9.4 | 0.540 | $6.06 \times 10^{-4}$ | 0.2703 |
| 55 | $Cs^{137}$ | 33 | 0.663 | $3.43 \times 10^{-3}$ | 0.2703 |
| 56 | $Ba^{133}$ | 10 | 0.085, 0.320 | $1.01 \times 10^{-3}$ | 0.2703 |
| 58 | $Ce^{144}$ | 0.795 | 0.030, 0.134 | $8.69 \times 10^{-5}$ | 0.2703 |
| 63 | $Eu^{152}$ | 5.3 | 0.30, 1.20 | $6.11 \times 10^{-4}$ | 0.2703 |
| 71 | $Lu^{171}$ | 1.644 | 1.00 | $2.13 \times 10^{-4}$ | 0.2703 |
| 73 | $Ta^{179}$ | 1.644 | 0.70 | $2.23 \times 10^{-4}$ | 0.2703 |
| 88 | $Ra^{226}$ | 1620 | 0.188 | $2.78 \times 10^{-1}$ | 0.2703 |

Isotopes selected are those with long half-lives and relatively high energy levels. The masses required are determined arbitrarily as those quantities which will produce $10^{10}$ disintegrations per second.

## Scintillation Detector and Its Uses

The device used by the interceptor to detect the gamma rays is called the scintillation detector. This detector works on the principle that when a gamma photon strikes a material called a phosphor, the phosphor emits a flash of light. This absorption of energy by a substance and its reemission as visible light is known as luminescence. The emitted light is proportional in intensity to the energy level of the photon. The detector is prevented from reacting to other types of equal-energy radiation particles by placing a shielding hood over the detector's head.

Figure 3a is a schematic diagram of a scintillation detector used as a gamma-ray counter. The emitted light is picked up by the sensitive photocathode of a photomultiplier tube producing a current pulse. This current pulse is similar to the light output from the phosphor crystal in both magnitude and duration. The current pulse produces a voltage pulse at the input of the preamplifier. This pulse, after passing the discriminator and pulse shaper, is counted by the electronic counter. Alternatively, the electronic counter can be replaced by a differential pulse-height analyzer to have a scintillation spectrometer.

The choice between the electronic counter or the pulse-height analyzer depends on the function of the scintillation detector. To determine the number of photons striking the phosphor crystal in a unit of time the electronic counter is used. This counting function is used to determine

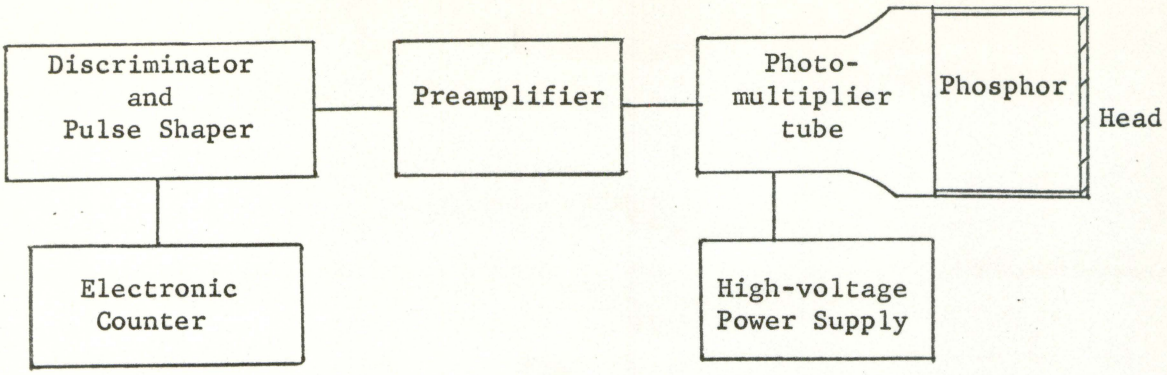


Figure 3a. Schematic diagram of a scintillation detector

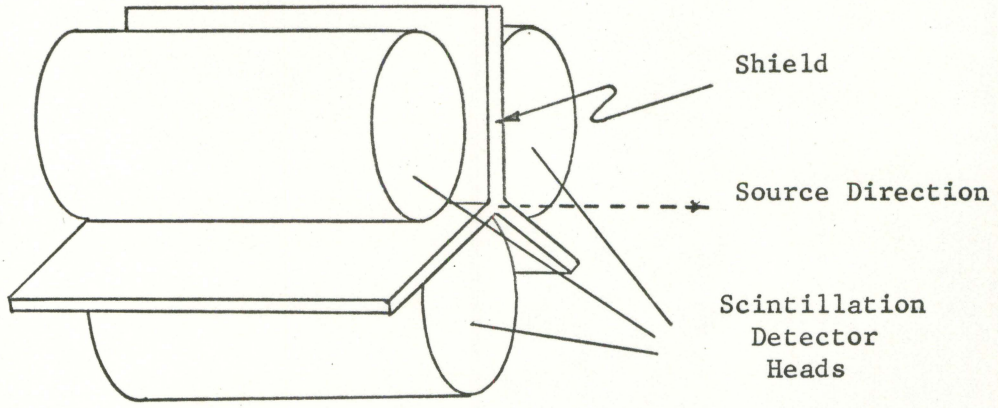


Figure 3b. Scintillation detector arrangement on a sensor

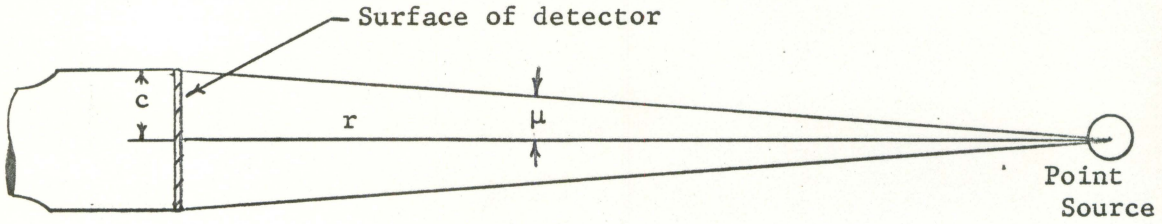


Figure 3c. Geometry between the scintillation detector and point source

the range r between the interceptor and target. The pulse-height analyzer is used to determine the energy levels of the detected photons. This identification function is used to determine the parameters $\alpha$, $\beta$, and $\gamma$ which are required to compute the relative position of the target to the interceptor.

As already shown, with four point sources of different gamma rays forming a rectangular pattern on the target, the interceptor can determine the target's relative position. The four point sources needed for this system fall into two categories. Points J and K (Figure 2b) are to provide $10^{10}$ gamma photons per second for range determination and have distinct energy levels. The significance of $10^{10}$ photons per second is discussed later in the section on range determination. Points L and M need only have distinct energy levels. They need only emit enough gamma rays per second so that they can readily be detected and followed from all required ranges.

## Angle Determination

Because there is a proportionality between the output pulse of the photomultiplier and the energy dissipated by the photons within the detector, it is possible to measure the energy of the nuclear particles. Measurements of this type are usually presented as energy distribution curves such as the ones shown in Figure 4. These curves are plots of the number of occurrences of photons with a specific energy striking the scintillation detector during a certain time versus the energy of the photons expressed in terms of voltage pulse-height. These energy-distribution curves are commonly known as spectra, and the equipment for

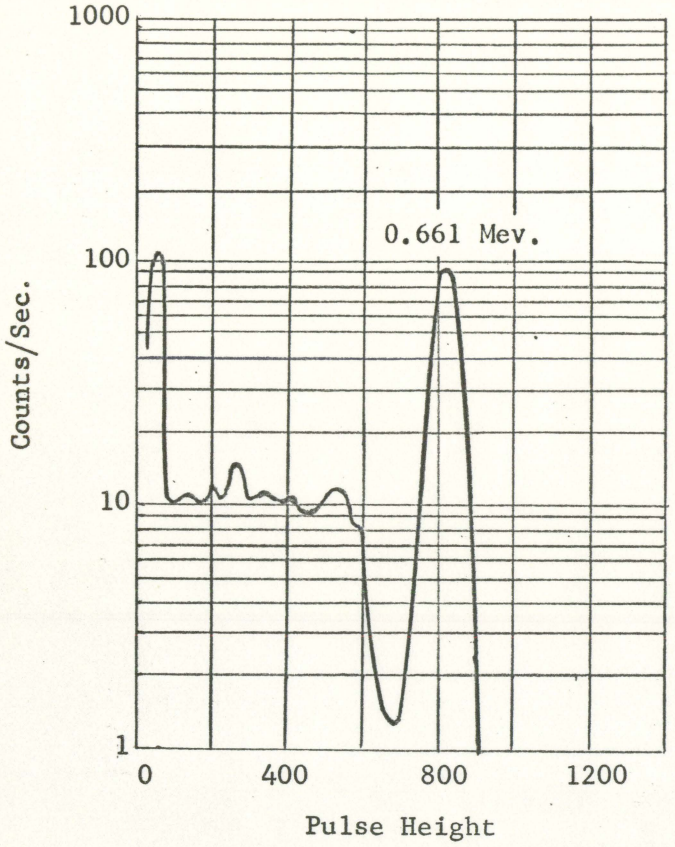


Typical $Cs^{137}$ gamma ray spectrum

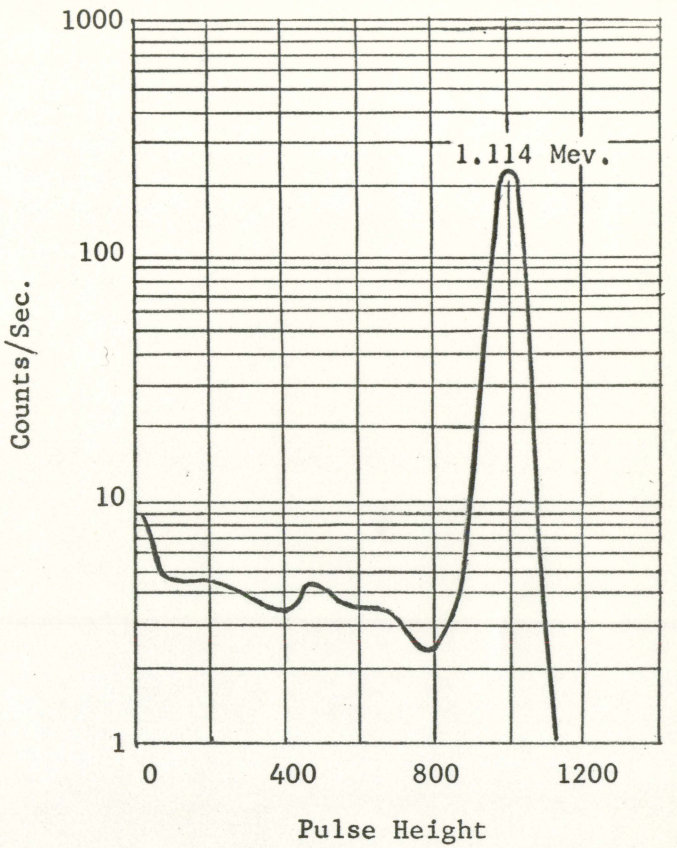


Typical $Zn^{65}$ gamma ray spectrum

Figure 4. Energy distribution curves

obtaining the curves is known as the spectrometer.

As seen in Figure 4, the energy-distribution curves of both materials have characteristic peaks. These peaks are known as the full-energy peaks and occur at the energy which is characteristic of the particular gamma-ray emitting material. Materials with more than one discrete energy level have more than one peak in their curves. The other energy levels present are due to the interaction of the photons with the crystal atoms causing some of the photon energy to be lost.

Spectrometers which employ crystals sufficiently large that most of the pulses appear under the full-energy curve are known as total-absorbtion spectrometers. Because photons of four energy levels react with each scintillation spectrometer, it is desirable that each be a total-absorbtion spectrometer. Then no energy peak will be lost in the secondary energy levels caused by the interactions of the other photons.

The pulse-height analyzer that is part of the scintillation spectrometer is made up of a multiple-channel network. Each channel measures a certain discrete energy band. By turning off all channels except those which measure the energy level of the desired gamma ray, the spectrometer can be made to recognize only this gamma ray. In other words, regardless of which gamma photons strike the scintillation detector, the only ones recorded are those with the energy level to which the analyzer is set.

When gamma rays from the four point sources on the target strike each of the interceptor's sensors they all cause the phosphors to emit light flashes. But each sensor's pulse-height analyzer is adjusted to recognize just one energy level. Therefore, only the flashes of light

of the right energy level are recorded. This is what is meant by having each sensor "tuned" to an energy level.

In addition to being able to record only gamma rays from a certain point source, it is desired that each sensor point directly to that point source. This can nearly be done by making each sensor have a group of three scintillation detectors arranged in a triangular pattern as shown in Figure 3b. The three detectors are separated by an extended shield made of a material which will not allow passage of all the gamma rays which strike it. Thus, if the sensor is not pointed directly toward the point source to which it is tuned each phosphor surface will measure different amounts of photons from that source. These different amounts of gamma rays cause a differential electrical signal to exist between the three detectors. This signal activates a positioning motor which aligns the sensor to where all three detectors receive the same number of photons per second. Thus, if the point source that emits a particular energy level of gamma rays is the only source present from which that energy level comes, the tuned sensor positions itself to point directly toward that point source.

Ideally, this method of angle determination yields correct values of the angles $\alpha$, $\beta$, and $\gamma$. However, because the point sources emit photons in an isotropic pattern, some of these photons go into the target vehicle and interact with the atoms of the materials in the vehicle. These photons are then emitted from the target vehicle with different energy levels. The incoming photons also cause further nuclear transformations of materials in the target releasing more gamma rays. This phenomenon is known as Compton scattering. A certain percentage of these photons which

are emitted in a random pattern from the target have the same energy level as the point sources.

The presense of these scattered photons cause some error in the direction which the sensors point. A conservative value of the amount of these random direction photons with the same energy level as those from a particular point source is 1%. This amount and the center of its location, when detected from the sensor on the interceptor, depends on the location of the interceptor to the target, the original energy level of the photons emitted from the point sources, the materials present in the target vehicle, and the geometry of the vehicle.

The actual amount of angle error caused by Compton scattering would be determined by testing the sensor in different positions relative to the target vehicle. In general, the effect of Compton scattering tends to make the locations of point sources J, K, L, and M appear, as detected from the interceptor, to be more toward the center of the target than they actually are. This would have little effect on the angle $\alpha$ but would decrease the values of $\beta$ and $\gamma$. A decrease in angles $\beta$ and $\gamma$ would tend to increase the calculated value of the y displacement component and to decrease the calculated value of the z component. The x component would be unaffected. These predictions are determined by inspection of Figure 2b. If required, the resulting angle errors can be decreased to an acceptable amount by increasing the shielding of the point sources from the target and by arranging the point sources with the lower energy sources in the front positions (points L and M).

The angular positions of the sensors are measured relative to their mounts on the interceptor by angle transducers. The interceptor's

attitude in turn is determined by referencing it to the stabilized platform on board. The angular turning rates of the sensors are measured by accelerometers.

## Range Determination

If a point source emits a certain number of photons per second, the number interacting with the scintillation detector is a function of the detector's range from the source. For this investigation, it is assumed that the point source emits $10^{10}$ gamma photons per second in an isotropic pattern. This number is chosen because it enables selecting reasonably sized scintillation detectors which yield the required measurement accuracy over the range desired. Only one sensor and point source are needed to determine range. The point source selected here is the one marked K in Figure 2b because the approach is assumed to occur from the -Y direction. Point source J has this capability from the +Y direction.

It is also arbitrarily assumed that the scintillation detector can count individually up to 10,000 photons per second which is a reasonable number considering present detectors available. Increasing this number increases the range span which the detector can determine. The total number of photons striking the detector at one time is proportional to the solid angle coming from the point source. This solid angle is a function of the range and the detector's shape.

The point sources are considered to be spherical. The surface area of a sphere enclosed by a circular cone with a half-angle of $\mu$ and the vertex at the sphere's center is

$$A = 2\pi R^2 (1 - \cos \mu) . \tag{41}$$

The total area of a sphere's surface is $4\pi R^2$ so the portion of the sphere's surface enclosed by the cone is

$$\frac{A}{A_{tot}} = \frac{2\pi R^2 (1 - \cos \mu)}{4\pi R^2}$$

$$= \frac{1 - \cos \mu}{2} . \tag{42}$$

For a round scintillation detector with a diameter 2c of distance r away from the point source, the arrangement is as shown in Figure 3c. The solid angle of gamma rays striking the detector forms a cone of half-angle $\mu$. Therefore, the ratio of gamma rays striking the detector to the total number of rays emitted is found by applying Equation 42.

$$\frac{A}{A_{tot}} = n = \frac{1 - \cos \mu}{2} ,$$

or

$$n = \frac{1 - \frac{r}{\sqrt{r^2 + c^2}}}{2} . \tag{43}$$

Solving this equation for range r gives

$$r = \frac{c(1 - 2n)}{2\sqrt{(n - n^2)}} . \tag{44}$$

By considering that the detector will count a maximum of 10,000 photons per second and that $10^{10}$ is the total number emitted per second, it is found that maximum ratio n is

$$n_{max} = \frac{10,000}{10^{10}} = 10^{-6} . \tag{45}$$

When this is put into Equation 44, r can be seen to be approximately

$$r \approx \frac{c}{2\sqrt{n}} . \tag{46}$$

This approximation enables determining the proper size scintillation detector depending on the accuracy required at a particular range.

The random error of gamma ray emission from the point source must also be taken into account. If N is the number of counts totalized over a time interval t, the counting rate $\dot{N}$ is

$$\dot{N} = \frac{N}{t} .$$

This value, with its standard deviation, may be stated as

$$\dot{N} \pm \sigma = \frac{N}{t} \pm \frac{N^{1/2}}{t} .$$

Stated in terms of percentage error, this is

$$\dot{N} \pm \frac{100\%}{N^{1/2}} .$$

For $\dot{N}$ = 100 counts per second, this is 100 $\pm$ 10% = 100 $\pm$ 10 counts per second. For $\dot{N}$ = 10,000 counts per second, this is 10,000 $\pm$ 1% = 10,000 $\pm$ 100 counts per second. It is seen that

$$\dot{N} = (10^{10})n,$$

where n is the ratio of emitted photons which strike the detector head.

As previously noted, the determination of range by using radar has an accuracy of $\pm$10 feet. This accuracy is adequate for the rendezvous guidance system. However there is a point when it is desirable that range accuracy become more accurate than this and improve as the range becomes smaller. For this discussion, this point in range is chosen to be 500 feet.

By a trial-and-error method it is found that with a point source emitting $10^{10}$ gamma rays per second, the size of the detector radius required at 500 feet to provide equivalent accuracy is 0.250 feet. This

is the value of c. From Equation 46, it is seen that

$$\sqrt{n} = \frac{c}{2r} = \frac{0.250}{1000} \text{ or } n = 6.25 \times 10^{-8}.$$

Then $\dot{N} = 625 \pm 25$ counts per second.

For $\dot{N} = 650$ counts per second,

$$r = \frac{0.250}{2\sqrt{6.50 \times 10^{-8}}} = 490.2 \text{ feet.}$$

For $\dot{N} = 600$ counts per second,

$$r = \frac{0.250}{2\sqrt{6.00 \times 10^{-8}}} = 510.2 \text{ feet.}$$

The radar range finder used by the rendezvous system is left operating until the interceptor reaches 500 feet. At this point the 0.25 foot radius scintillation detector is put into use. Although its accuracy at this point is also about $\pm 10$ feet as shown, it improves as range diminishes. This detector is used until the point is reached where it records 10,000 counts per second. This range if found to be $125 \pm 0.6$ feet.

At 125 feet the task of range determination is switched to a second detector which is large enough to record 1600 counts per second at this range. Its radius is

$$c = 2r\sqrt{n} = 2\ (125)\ \sqrt{1.6 \times 10^{-7}}$$

$$= 0.100 \text{ feet.}$$

This detector's accuracy at this point is expressed as

$$r = 125\ {}^{+1.6}_{-1.5} \text{ feet.}$$

This second detector is used to determine range until the interceptor is 50 feet from the target, where 10,000 counts per second are again

recorded. The system used for measuring range from 50 feet to zero will be explained later.

Two of the six sensors with the triangularly arranged scintillation detectors mentioned before that are used for position sensing of point sources, also serve as range finders. One detector on each of these two sensors has a 0.250 foot radius. Another detector on each has a 0.100 foot radius. These two detectors used in succession determine range as previously explained. All three detectors on each sensor continuously work together to determine direction of the point source. This is done by having a proportionality factor based on the phosphor crystal size built into the sensor electronics to account for different amounts of energy measured by the different crystal sizes.

The advantage of using the scintillation detector to determine range is plainly seen. The detector complements the previously used radar system because it becomes more accurate as range decreases.

This system of range detection has a good deal of flexibility. For this discussion the scintillation detectors with electronic counters are used to measure range from 500 feet to 50 feet. This range span can be changed by changing detector sizes and the number of gamma rays emitted per second by the point sources. These changes depend on the maneuver conditions that the interceptor must go through and the accuracy of range required.

It must be pointed out that there is a maximum and a minimum size to the scintillation detectors that can be used in this system. The maximum limit results from the fact that phosphor crystals are limited in the size that can be made. Also, the greater the size of the detector,

the more unwieldly it becomes on a gimbaled sensor. The minimum size is dictated by two facts. The photomultiplier tube must have a certain minimum size to be able to count 10,000 counts per second. The detector also has a minimum size because discrete energy levels become more and more broken down and scattered as the detector's head becomes smaller and smaller.

To determine the interceptor's range rate or relative velocity, Equation 44 is differentiated with respect to time.

$$\dot{r} = \frac{d}{dt}\left(\frac{c(1 - 2n)}{2(n - n^2)^{1/2}}\right) \tag{47}$$

$$= \frac{-4c\ (n - n^2)\ \dot{n} - c\ (1 - 2n)^2\ \dot{n}}{4(n - n^2)^{3/2}} . \tag{48}$$

This is approximately

$$\dot{r} = -\frac{c\dot{n}}{4n^{3/2}} , \tag{49}$$

which is the same result as differentiating the range approximation, Equation 46, with respect to time.

## DOCKING MANEUVER CONTROL

The information the interceptor requires to determine its relative position and velocity with respect to the target space station has been specified. The sensors which determine this information have been described. Now required is a method by which the interceptor can use the position and velocity information as inputs to a command system to enable the interceptor to dock on the target.

There are several different directions from which the interceptor can dock on the target. The most probable alignment, at least for early missions, would be to have the roll axis of the interceptor align parallel to the X axis of the target. It has been assumed here that this alignment is made from the -X direction.

Referring to Figure 3 it can be seen that there are two evident ways which the interceptor can use to close the range between itself and the target. They are:

1. The interceptor can be driven along the line-of-sight between itself and the target. This is similar to the previous technique of rendezvousing. This approach has the advantage that the interceptor is already equipped for this type of path control.

2. The interceptor can be driven to the X axis and then made to close the distance x at some nominal velocity. This implies that the y and z components of displacement are driven to zero by the time x reaches some given value.

The latter method of docking is chosen here because it provides a

capability that allows a more maneuverable docking sequence.

Because the interceptor can determine the X, Y, and Z directions it can align its roll, pitch, and yaw axes parallel to these directions. This is done by the interceptor making proper angular alignments $\Phi$ and $\Theta$ to the line-of-sight direction. This alignment occurs automatically so that velocity correcting thrusts from the interceptor engines are in the correct directions.

The relative velocity between the interceptor and target has been shown to be

$$\dot{\bar{r}} = (\dot{x} - \omega z)\bar{e}_i + \dot{y}\bar{e}_j + (\dot{z} + \omega x)\bar{e}_k \ . \tag{7}$$

If this expresses a constant velocity for an increment of time then it can be integrated over that period of time to determine the change in range.

$$\int_{t_o}^{t_1} \dot{\bar{r}}dt = \int_{t_o}^{t_1} \left[(\dot{x} - \omega z)\bar{e}_i + \dot{y}\bar{e}_j + (\dot{z} + \omega x)\bar{e}_k\right] dt, \tag{50}$$

or

$$\bar{r}_1 - \bar{r}_o = \left[(\dot{x} - \omega z)\bar{e}_i + \dot{y}\bar{e}_j + (\dot{z} + \omega x)\bar{e}_k\right]\left[t_1 - t_o\right], \tag{51}$$

where $\bar{r}_1$ = range at $t_1$,

$\bar{r}_o$ = range at $t_o$.

If velocity remained constant at the values measured at time $t_o$, Equation 51 would represent ideally the change in range over some general time period t. However, in the actual docking sequence, time must be allowed for retrothrusts, angular alignment of the interceptor, and various system delays. To incorporate this additional time the right hand side of Equation 51 is divided by a gain constant k and the

general expression for change in range becomes

$$\bar{r} - \bar{r}_o = \frac{1}{k}\left[(\dot{x} - \omega z)\bar{e}_i + \dot{y}\bar{e}_j + (\dot{z} + \omega x)\bar{e}_k\right]t. \tag{52}$$

Equation 52 can be broken into position components for some general time t.

$$x = x_o + \frac{(\dot{x} - \omega z)t}{k} . \tag{53}$$

$$y = y_o + \frac{\dot{y}t}{k} . \tag{54}$$

$$z = z_o + \frac{(\dot{z} + \omega x)t}{k} . \tag{55}$$

Because of propellant limitations and other factors, the docking maneuver is required to take place in a definite time T'. For this docking system, it is required that $x = C_1$, $y = 0$, and $z = 0$ in the time period T' after the docking maneuver has begun. $C_1$ is the separation distance along the X axis. These values are substituted into Equations 53, 54, and 55 to yield

$$C_1 = x_o + \frac{(\dot{x} - \omega z)T'}{k} , \tag{56}$$

$$0 = y_o + \frac{\dot{y}T'}{k} , \tag{57}$$

$$0 = z_o + \frac{(\dot{z} + \omega x)T'}{k} \tag{58}$$

These equations represent the ideal case considered at the point when the interceptor is at $\bar{r}_o = x_o\bar{e}_i + y_o\bar{e}_j + z_o\bar{e}_k$, and there is time T' left to enact the maneuver.

The situation that prevails after a time period t can be found by subtracting Equations 56, 57, and 58 from 53, 54, and 55.

Motion is considered along the Z axis by subtracting Equation 58 from Equation 55.

$$z = z_o + \frac{(\dot{z} + \omega x)t}{k} - z_o - \frac{(\dot{z} + \omega x)T'}{k}, \tag{59}$$

or

$$z = \frac{(\dot{z} + \omega x)(t - T')}{k}. \tag{60}$$

Solving Equation 60 for the ideal velocity $\dot{z}$ after a time $(T' - t)$ has elapsed yields

$$\dot{z} = \dot{z}_i = \frac{-kz}{(T' - t)} - \omega x. \tag{61}$$

The subscript i means that this is an expression of the ideal velocity. The value of directional velocity expressed in Equation 61 represents the ideal velocity required at the time t when position components z and x are measured and z is required to be zero at time $(T' - t)$ seconds later. This ideal velocity represents a reference to which the actual velocity of the interceptor in the Z direction at time t can be compared.

In the same manner, ideal velocities in the X and Y directions are found to be

$$\dot{x}_i = \frac{-k(x - C_1)}{(T' - t)} + \omega z, \tag{62}$$

$$\dot{y}_i = \frac{-ky}{(T' - t)}. \tag{63}$$

Because $x_i$ is not necessarily zero at time T', Equation 62 is modified to include a nominal closing velocity $C_2$.

$$\dot{x}_i = C_2 - \frac{k(x - C_1)}{(T' - t)} + \omega z. \tag{64}$$

Equations 61, 63, and 64 represent velocities which guarantee that the interceptor will be in the correct position and moving at the correct velocity at time T'. The commands that activate the control engines are made by comparing these ideal velocities to the actual measured velocities. If an error exists between the ideal and actual velocity that exceeds some value $V_e$, the vernier control engines are activated to make the corrections in the required directions. If the error is less than $V_e$ the engines are deactivated. The existence of the error margin velocity $V_e$ prohibits the control engines from switching on and off, or hunting around the ideal velocity. Also, the thrust engines are prohibited from firing if they are not aligned within certain limits of the command direction.

Thus if $\left|\dot{x}_i - \dot{x}\right| > V_e$ the X direction rockets are turned on in the correct direction. Thrust in the X direction, as developed in Equation 12, is

$$\frac{T_x}{m_p} = \ddot{x} - 2\omega\dot{z} - \omega^2 x, \tag{12}$$

or

$$\ddot{x} = \frac{T_x}{m_p} + 2\omega\dot{z} + \omega^2 x. \tag{65}$$

From these, a close approximation of the time for the X direction engines to be on is found to be

$$t = \frac{\left|\dot{x}_i - \dot{x}\right|}{\ddot{x}} = \frac{\left|\dot{x}_i - \dot{x}\right|}{\frac{T_x}{m_p} + 2\omega\dot{z} + \omega^2 x}. \tag{66}$$

Similar equations can be developed for the time of thrust in the Y and Z directions using Equations 13 and 14.

Therefore, a program is established which assures that docking will occur. The gain constant k must be chosen (based on thrust available) so that there is sufficient time for all maneuvers to occur while attaining the docking path.

An advantage to this type of guidance system is that the interceptor can be made to approach the target along any specified direction. This is accomplished by putting the proper position constants in Equations 56, 57, and 58. The required closing velocity is attained by adding the proper component constants to Equations 61, 62, and 63.

## FINAL APPROACH

The preceding system is established so that when $x = C_1$, the y and z components of displacement are driven to zero. Also, at this point, the nominal closing velocity between the two vehicles is established as $\dot{x} = C_2$. Now, it remains to define a system which will guide the interceptor until contact and final lockon with the target is made.

It is remembered that the 0.100 foot radius scintillation detector discussed in the section about range determination reaches its lower limit as a range detector when range equals 50 feet. This is the range value where 10,000 gamma rays per second hit the detector phosphor crystal. Therefore, a new system of range measurement must take over from this point on in.

The value of $C_1$ in the steering equations, where the values of y and z are zero, is made equal to -50 feet. Then, from $x = -50$ on in, it can be assumed that the lateral displacements y and z will be quite small. This assumption allows small angle approximations to be made. Then the range value r is approximately equal to -x.

Again, use is made of the detectors that seek out and follow individual point sources. By referring to Figure 2, it is seen that

$$x = -r = -l_1 \cot \beta, \tag{67}$$

$$\dot{x} = l_1 \csc^2 \beta \, \dot{\beta}, \tag{68}$$

where $l_1$ is the distance between point sources J and K. $\beta$ is the angle between the sensors which seek points J and K. Thrusts in the roll axis direction can make the corrections necessary between the desired closing velocity $C_2$ and that measured by Equation 68.

For perfect alignment of the interceptor roll axis with the middle of the target vehicle, the point source J should align with point source L as viewed from the interceptor. Likewise, point sources K and M should align. Any lateral deviation can easily be determined by angular differences in the sensors tracking these pairs of point sources. The direction of the deviation can also be readily determined for it is the same as the direction of the line JL or KM as detected from the interceptor.

This final approach step is included to provide a time to correct errors that exist in closing velocity and angular alignment. Restricting the approach to have a final check at -50 feet builds in a safety factor for the mission. If some component of the interceptor malfunctions during the rendezvous and docking procedure, the interceptor can go crashing into the target vehicle which could be disasterous. With the check in position at -50 feet and the subsequent vernier control phase, the capability exists of either making a new docking attempt or aborting the mission.

## RESULTING GUIDANCE SYSTEM

The resulting docking guidance system developed in this investigation is shown in block diagram form in Figure 5. The sensors determine range r and the angular values $\alpha$, $\beta$, and $\gamma$ which exist between directions of the point sources on the targets. These four parameters are inputs to the coordinate computer. The angular attitudes of the sensors on the interceptor are also determined and sent as inputs to the attitude control system.

The coordinate computer determines angles $\theta$ and $\phi$ by Equations 20 and 36. These two angles are used with range r to calculate x, y, and z by Equations 15, 16, and 17. The velocity components $\dot{x}$, $\dot{y}$, and $\dot{z}$ are found by measuring the time rate of change of x, y, and z. From the coordinate computer, inputs of $\theta$ and $\phi$ are sent to the attitude control system. The velocities $\dot{x}$, $\dot{y}$, and $\dot{z}$ are sent to a comparator. The position components are inputs to the velocity command computer.

The velocity command computer calculates ideal velocities by Equations 61, 63, and 64. These ideal velocities are also sent as inputs to the comparator.

The attitude control system computes the angles that the interceptor's pitch and yaw axes make to the line-of-sight. These are found by measuring the sensors' gimbal angles to the interceptor's axes and the interceptor's attitude to a stabilized platform. When these angles are determined, they are compared to components of angles $\theta$ and $\phi$. The differences are attitude errors of the interceptor. These errors are sent as signals to the propulsion system which is activated to correct them.

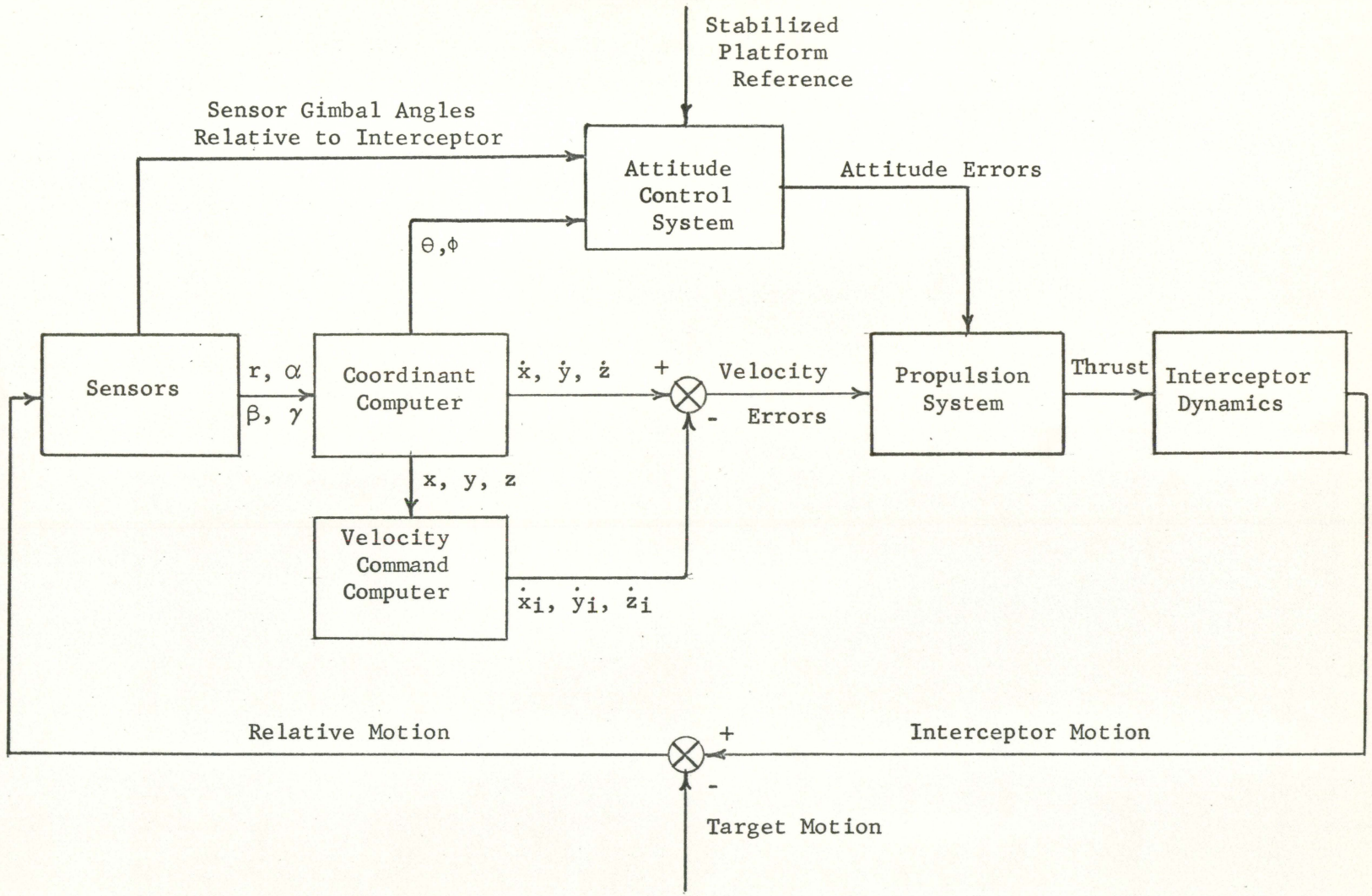


Figure 5. Block diagram of docking guidance system

The velocity comparator measures the velocity errors. These errors are also sent as signals to the propulsion system where correcting reactions take place.

The propulsion system makes attitude corrections first. When the interceptor attitude is acceptable, velocity corrections are made by use of equations such as Equation 66. Constant thrust engines are adequate for the propulsion system.

Thus, the entire system is coordinated so that it can take the random position and velocity conditions and use them as signals to direct the docking maneuver. The sequence of events which take place among the interdependent guidance and control subsystems are programmed so that the desired motion of the docking maneuver results. Proper gain constants, time delays, and error margins are found by analysis of each subsystem so that the optimum response of the entire system takes place.

## SUMMARY AND CONCLUSION

The problem of devising an automatic docking guidance system was studied by dividing it into two questions. They are:

1. How can an interceptor determine its position relative to the target?
2. How can the interceptor use the values of position components as signals with which to guide itself to the target?

In answering the first question, use was made of a principle from solid mechanics: The relative position of a rigid body to an exterior point can be defined by determining the relative positions of three non-linear points within that body to the point. Thus, by placing three point sources of gamma radiation on the target satellite, it was shown that the interceptor was able to determine the relative position coordinates by using scintillation detectors. It was necessary to have four point sources on the target so that this method would function from either side of the target.

To answer the second question, the relative velocity equation was transformed into ideal velocity component equations for the three cartesian directions as defined from the target vehicle. These ideal velocities are functions of the position components and the time remaining for the docking maneuver to be accomplished. Therefore, by having the control system correct the errors between the ideal and actual velocity components, the interceptor can be guided to dock with the target.

As is true in the evaluation of any system, there are advantages and

limitations that must be considered. Of course, the overall advantage of having a special guidance system for the docking phase alone is evident when the risks of not having one are considered. If the less accurate radar system used for the terminal rendezvous phase were extended to be the docking guidance system, heavy structural tolerances would have to be built into both the interceptor and the target vehicles to withstand the random final impact. On the other hand, the proposed guidance system not only provides for a soft, accurate docking maneuver but provides for a position check point so that a malfunction of the docking guidance system can be found before a damaging collision is made.

It has been suggested in the literature (9) that optical sensing devices might be employed as basic sensors for the docking maneuver. These sensors could use the same principles as the scintillation detectors, each seeking different color or modulation frequency light sources. The disadvantage of the optical sensor, however, is that the point sources of light on the target must be on for a long period of time and must also remain at constant energy levels over this period of time. Such a system would cause a large electrical power loss from the satellite. Otherwise, there must be some device on the target to turn the lights on and off at the required times which might have questionable reliability.

The merit of using the scintillation detector as the basic sensor is that all operating electrical parts of the guidance system are on the interceptor. Although the point sources emit gamma rays continuously, they are not dependent on any other process taking place on the target. Thus, docking can always take place even if there would be a power unit failure on the target.

There are certain regions of the Van Allen radiation belts where docking could not take place using the scintillation detector. In these regions there are dense, high-energy protons and electrons from which the detectors could not be adequately shielded; the particles would saturate the detector at all energy levels so that no measurements could be made. Therefore, the orbit path of the target vehicle would have to be planned so that docking could take place outside of these regions.

The scintillation detectors' measurement accuracies would also be affected by the activity of the sun. During the times of large solar flares, dense quantities of multi-energy photons exist around the earth which would cause the detectors to be non-functional as docking guidance sensors. However, periods of time can be predicted when solar activity is negligible so that docking can take place. Because a small solar flare can exist at random which would momentarily saturate the interceptor's scintillation detectors, the interceptor must be able to sense these occurrences. Then the docking maneuver can be temporarily delayed until such radiation passes.

An obstacle confronting the use of an automatic docking system employing gamma radiation detection is the cost of developing a detector with enough precision to yield the required accuracy. Also, tests must be run to develop the system which keeps errors caused by Compton scattering and random photon outputs at a minimum. However, with the advent of the recoverable ferry vehicle, the initial cost of developing the docking guidance system can be spread over a long period of usage. Then, when considered with the increased chance of repeated mission success, the foregoing development of a docking guidance system using

the scintillation detector seems quite reasonable.

In conclusion, the result of this investigation has been the determination of a feasible technique which can be utilized to fill the need for an automatic space docking guidance system. The development of this guidance system would allow the building of very elaborate space satellites, for it can be seen that placement of these point sources could be easily varied in location on the target. Also, the maneuverability of the interceptor makes it possible to build onto the satellite from any direction. The most important factor is that this can be done accurately without requiring the presence of man.

## RECOMMENDATIONS FOR FURTHER STUDY

This preliminary study of a docking guidance system was partially based on the assumption that the scintillation detector could be developed as the sensor for determining relative position between the interceptor and target vehicles. The next logical step is to test a group of scintillation detectors to find out if they could successfully determine the location of a point source of gamma radiation. Further testing would be required to decide whether or not the theory of using three sensors (composed of scintillation detectors) to determine the relative position components of a satellite is workable. If these tests demonstrate that gamma-ray detection can provide the degree of measurement accuracy required, then it can be said that the system developed within this paper provides a definite means of docking guidance.

Further analysis of the docking guidance system proposed in this study is necessary to determine the type of controls necessary. Study is also necessary to determine gain constants, time delays, error margins, and other factors of each subsystem which influence the success of the docking maneuver. System analyses of the control and propulsion systems and their effects on the guidance system provide further areas of necessary research.

A final step for verification of the feasibility of this docking guidance system would be to define mathematically all subsystems of which it is composed. Then a computer study, in which each subsystem is simulated, could be made. In this way, the entire guidance system could be analyzed to determine whether it is adequate to direct the docking

maneuver with variable input conditions. Also, design change ideas could then be analyzed to arrive at the optimum system.

Many related areas of study concerning docking remain which depend on the design of the vehicles involved. These include the study of the design of possible latching devices, structural requirements of the uniting vehicles, and design of automatic methods for transferring cargo. Another investigation which can use the principles developed in this thesis is that of a guidance system required to maintain the interceptor at a fixed position away from the target or to cause the interceptor to rotate around the target for inspection purposes.

## LIST OF REFERENCES


1. Carney, Terrance M. An automatic terminal guidance system for rendezvous with a satellite. National Aeronautics and Space Administration Technical Note D-923. 1961.

2. Farless, D.L. and Caggiano, G. Techniques for rendezvous and docking. Advances in the Astronautical Sciences 16, Part 1: 94-114. 1963.

3. Glasstone, Samuel. Sourcebook on atomic energy. Princeton, N.J., D. Van Nostrand Co., Inc. 1950.

4. Grubin, Carl. Docking dynamics for rigid-body spacecraft. American Institute of Aeronautics and Astronautics Journal 2: 5-12. 1964.

5. Harrison, Eugene. Rendezvous energy required for collision and pursuit course guidance. Advances in the Astronautical Sciences 16: 77-93. 1963.

6. Harshaw Chemical Company. Harshaw scintillation phosphors. 2nd ed. Cleveland, Ohio, author. 1962.

7. Heilfron, J. and Kaufman, F.H. Rendezvous and docking techniques. Progress in Astronautics and aeronautics 10: 237-264. 1963.

8. Hodgman, C.D., ed. Handbook of chemistry and physics. 38th ed. Cleveland, Ohio, Chemical Rubber Publishing Co. 1956.

9. Irish, Leslie A. Guidance equations for automatic docking. Advances in the Astronautical Sciences 16, Part 1: 3-15. 1963.

10. McCuskey, S.W. Introduction to advanced dynamics. Reading, Mass., Addison-Wesley Publishing Co., Inc. 1962.

11. Montgomery, James E. Manned control of space vehicle docking. Advances in the Astronautical Sciences 16, Part 1: 147-161. 1963.

12. Price, William J. Nuclear radiation detection. New York, N.Y., McGraw-Hill Book Co., Inc. 1958.

13. Redmond, Robert F. Space radiation and its effects on materials. Battelle Memorial Institute, (Columbus, Ohio). Radiation Effects Information Center Memorandum 21. 1961.

14. Roberson, Robert E. Analytical considerations of space rendezvous. Progress in Astronautics and Aeronautics 10: 211-236. 1963.

15. Semiconductors, scintillators, and pulse-height analyzers. Nucleonic 20, No. 5: 53-55. May 1962.

16. Shapiro, M. Attenuated intercept satellite rendezvous system. American Rocket Society Journal 31: 1733-1744. 1961.

17. Siegbahn, Kai, ed. Beta- and gamma-ray spectroscope. New York, N.Y., Interscience Publishers, Inc. 1955.

18. Steffon, Kenneth F. Satellite rendezvous terminal guidance system. American Rocket Society Journal 31: 1516-1521. 1961.

19. Ward, J.W. and Williams, H. M. Orbital docking dynamics. American Institute of Aeronautics and Astronautics Journal 1: 1360-1364. 1963.

20. Wolff, Jay R. and Ravanesi, Ralph M. Multichannel analyzers in space. Nucleonics 20, No. 10: 58-60. Oct. 1962.

21. Wolverton, Raymond W., ed. Flight performance handbook for orbital operations. New York, N.Y., John Wiley and Sons, Inc. 1963.

## ACKNOWLEDGEMENTS

I wish to express my appreciation to Dr. Glenn Murphy for the suggestion of using the scintillation detector in this problem and for his guidance and encouragement throughout the study. I would also like to thank Mrs. Janice Millard for the typing of this thesis. Finally, I wish to acknowledge my wife, Susan, who has helped in many ways.